ORIGINAL RESEARCH

Synthesis of composite magnetic nanoparticles Fe$_3$O$_4$ with alendronate for osteoporosis treatment

Ming-Song Lee[1,2]
Chao-Ming Su[1]
Jih-Chao Yeh[1,3]
Pei-Ru Wu[4]
Tien-Yao Tsai[1]
Shyh-Liang Lou[1,2]

[1]Department of Biomedical Engineering, [2]Department of Nanotechnology, Chung Yuan Christian University, Taoyuan, Taiwan; [3]Institute of Urology, University of Southern California, Los Angeles, CA, USA; [4]Department of Biomedical Sciences, College of Medicine, Chang Gung University, Taoyuan, Taiwan

Abstract: Osteoporosis is a result of imbalance between bone formation by osteoblasts and resorption by osteoclasts (OCs). In the present study, we investigated the potential of limiting the aggravation of osteoporosis by reducing the activity of OCs through thermolysis. The proposed method is to synthesize bisphosphonate (Bis)-conjugated iron (II, III) oxide (Fe$_3$O$_4$) nanoparticles and incorporate them into OCs. The cells should be subsequently exposed to radiofrequency (RF) to induce thermolysis. In this study, particles of Fe$_3$O$_4$ were first synthesized by chemical co-precipitation and then coated with dextran (Dex). The Dex/Fe$_3$O$_4$ particles were then conjugated with Bis to form Bis/Dex/Fe$_3$O$_4$. Transmission electron microscopy revealed that the average diameter of the Bis/Dex/Fe$_3$O$_4$ particles was ~20 nm. All three kinds of nanoparticles were found to have cubic inverse spinel structure of Fe$_3$O$_4$ by the X-ray diffraction analysis. Fourier transform infrared spectroscopy confirmed that the Dex/Fe$_3$O$_4$ and Bis/Dex/Fe$_3$O$_4$ nanoparticles possessed their respective Dex and Bis functional groups, while a superconducting quantum interference device magnetometer measured the magnetic moment to be 24.5 emu. In addition, the Bis/Dex/Fe$_3$O$_4$ nanoparticles were fully dispersed in double-distilled water. Osteoblasts and OCs were individually cultured with the nanoparticles, and an MTT assay revealed that they were non-cytotoxic. An RF system (42 kHz and 450 A) was used to raise the temperature of the nanoparticles for 20 minutes, and the thermal effect was found to be sufficient to destroy OCs. Furthermore, in vivo studies verified that nanoparticles were indeed magnetic resonance imaging contrast agents and that they accumulated after being injected into the body of rats. In conclusion, we developed a water-dispersible magnetic nanoparticle that had RF-induced thermogenic properties, and the results indicated that the Bis/Dex/Fe$_3$O$_4$ nanoparticle had the potential for controlling osteoporosis.

Keywords: iron oxide, thermotherapy, bisphosphonate, radiofrequency, thermolysis

Introduction

Osteoporosis is considered a silent killer due to its lack of symptoms and is often diagnosed only after the patient suffers a bone fracture. There are >54 million people with osteoporosis or reduced bone mass in the US alone, and by 2025, osteoporosis is projected to contribute to approximately three million bone fractures per year.[1] The drugs used to treat osteoporosis include bisphosphonate (Bis), strontium ranelate, calcitonin, and RANKL inhibitors.[2–5] Among these drugs, Bis is most commonly prescribed because it can combine with hydroxyapatite to inhibit farnesyl pyrophosphate synthase and reduce osteoclast (OC) resorption and bone turnover.[6] Alendronate is a potent nitrogen-containing Bis which has been widely prescribed for osteoporosis treatment. Some benefits of alendronate include inhibition of the absorption of bone

Correspondence: Shyh-Liang Lou
Department of Biomedical Engineering, Chung Yuan Christian University, No 200, Zhongbei Rd, Zhongli District, Taoyuan City, Taiwan 320
Email pacslou@gmail.com

matrix by OCs and retardation of the loss of bone calcium.[7] In the past 10 years, research has showed that alendronate can effectively limit aggravation of osteoporosis.[8–10] Though it has several advantages, side effects such as nausea, vomiting, and abdominal discomfort remain a concern.[11,12] Novel drug delivery systems such as nanoparticles, micelles, and liposomes can be used to enhance drug stability and efficacy while reducing the side effect of Bis.[13–15]

There has been a flood of novel nanoparticle therapies researched in recent years. In 1981, Massart successfully synthesized magnetic iron (II, III) oxide nanoparticles by employing an aqueous chemical co-precipitation method, and in the past decade, there has been widespread synthesis of magnetic nanoparticles conjugated with a variety of drugs.[16,17] Iron (II, III) oxide (Fe_3O_4) nanoparticles have a high magnetic field, and are chemically stable, nontoxic, and cost-efficient for applications such as hyperthermia treatment, drug delivery, cell isolation, and stem cell tracking, and can be used as magnetic resonance imaging (MRI) contrast agents.[18] One drawback, however, is that they can spontaneously aggregate and cause vessel embolism after intravenous application.[19] To address this problem, surfactants and polymers are commonly used in conjunction with the nanoparticles.[20] One example is dextran (Dex), a polysaccharide composed of long chain of glucose molecules. Since Dex is water soluble, pH neutral, biocompatible, biodegradable, and chemically stable, it is capable of improving Fe_3O_4 dispersion.[21] Another feature of magnetic nanoparticles is that they can increase the surrounding temperature when exposed to radiofrequency (RF). As a result, there is growing interest in using the nanoparticles for cell-specific thermolysis as a noninvasive therapeutic agent.[22,23]

Thermotherapy is an attractive treatment for osteoporosis because it can cause cell death by disrupting cell membranes and denaturing intracellular proteins.[24–27] Furthermore, the specificity of thermolysis ensures a safe treatment that prevents damage to the surrounding tissues.[28–30] The goal of this study is to control osteoporosis aggravation by destroying OCs through thermolysis. Fe_3O_4 nanoparticles were first synthesized by chemical co-precipitation and then coated with Dex.[31] The Dex/Fe_3O_4 particles were subsequently conjugated with Bis to form Bis/Dex/Fe_3O_4. Bis has a strong adherence to skeleton; thus, there is an increased likelihood for OCs to engulf the Bis/Dex/Fe_3O_4 nanoparticles. The side effects of Bis, as discussed earlier, are mostly caused by amidogen.[2] This study proposes removing the amidogen and grafting Dex/Fe_3O_4 to hydroxyl phosphonobutyl, to form Bis/Dex/Fe_3O_4. The proposed method is to synthesize Bis-conjugated Fe_3O_4 nanoparticles that will be engulfed by OCs, which will in turn be lysed by the temperature increase induced by RF exposures.

Materials and methods

All chemicals and reagents were used without further purification, and all the aqueous solutions were prepared using arium® 611 (18.4 MΩ cm⁻¹; Sartorius AG, Göttingen, Germany). Ferrous chloride tetrahydrate ($FeCl_2·4H_2O$), ferrous chloride hexahydrate ($FeCl_3·6H_2O$), Dex (($C_6H_{10}O_5)_n$, molecular weight [MW] ~40,000 Da), hydrazine (N_2H_4), sodium hydroxide (NaOH), sodium chloroacetate ($C_2H_2ClO_2·Na$), 1-ethyl-3-(3-dimethylaminopropyl) carbodiimide (EDC) hydrochloride ($C_8H_{17}N_3·HCl$), N-hydroxysuccinimide ($C_4H_5NO_3$; NHS), and alendronate sodium trihydrant ($C_4H_{12}NO_7P_2Na·3H_2O$) were all purchased from Sigma-Aldrich Co. (St Louis, MO, USA) and then used, as received, to synthesize the composite nanoparticles.

Reagents used in cell culture include albumin solution from bovine serum (Sigma-Aldrich Co.), ascorbic acid ($C_6H_8O_6$; Sigma-Aldrich Co.), Dulbecco's Modified Eagle's Medium (DMEM; high glucose with L-glutamine and pyridoxine hydrochloride; GibcoÒ; Thermo Fisher Scientific, Waltham, MA, USA), alpha-minimum essential medium (GibcoÒ; Thermo Fisher Scientific), sodium bicarbonate ($NaHCO_3$; Sigma-Aldrich Co.), hydrochloric acid (HCl; 36.5%–38%; J.T. BakerÒ; Avantor Performance Materials, Center Valley, PA, USA), penicillin (10,000 units/mL; Gibco), streptomycin (10,000 μg/mL; Gibco), recombinant mouse RANKL/Trance (R&D systems, Inc., Minneapolis, MN, USA), dimethyl sulfoxide (>99%; J.T. BakerÒ; Avantor Performance Materials), phosphate-buffered saline (PBS; potassium phosphate [KH_2PO_4; Sigma-Aldrich Co.], potassium chloride [KCl; Sigma-Aldrich Co.], sodium phosphate dibasic [Na_2HPO_4; Sigma-Aldrich Co.], sodium chloride [NaCl; Sigma-Aldrich Co.]), and 3-(4,5-dimethylthiazole-2-yl)-2,5-diphenyl tetrazolium bromide (MTT; Sigma-Aldrich Co.). All products and liquids were prepared in laminar flow under sterile conditions. All animal studies were performed with the approval of Institutional Animal Care and Use Committee and followed the guidelines of the Council of Agriculture, Taiwan.

Preparation of magnetic nanoparticles
Preparation of Dex/Fe_3O_4 magnetic nanoparticles
The particles were prepared by co-precipitation with hydrazine hydrate (Figure 1A, left). Prior to synthesis, a 250 mL three-neck flask was degassed with nitrogen for 30 minutes. Thirty milliliters of double-distilled water was injected into the flask at 80°C under mechanical stirring during the entire experiment. Ferrous chloride hexahydrate and Dex were mixed, while 10 mL of double-distilled water was injected into the flask for 5 minutes. Then, 0.835 mL of hydrazine was added into the reactant mixture to reduce particle size and
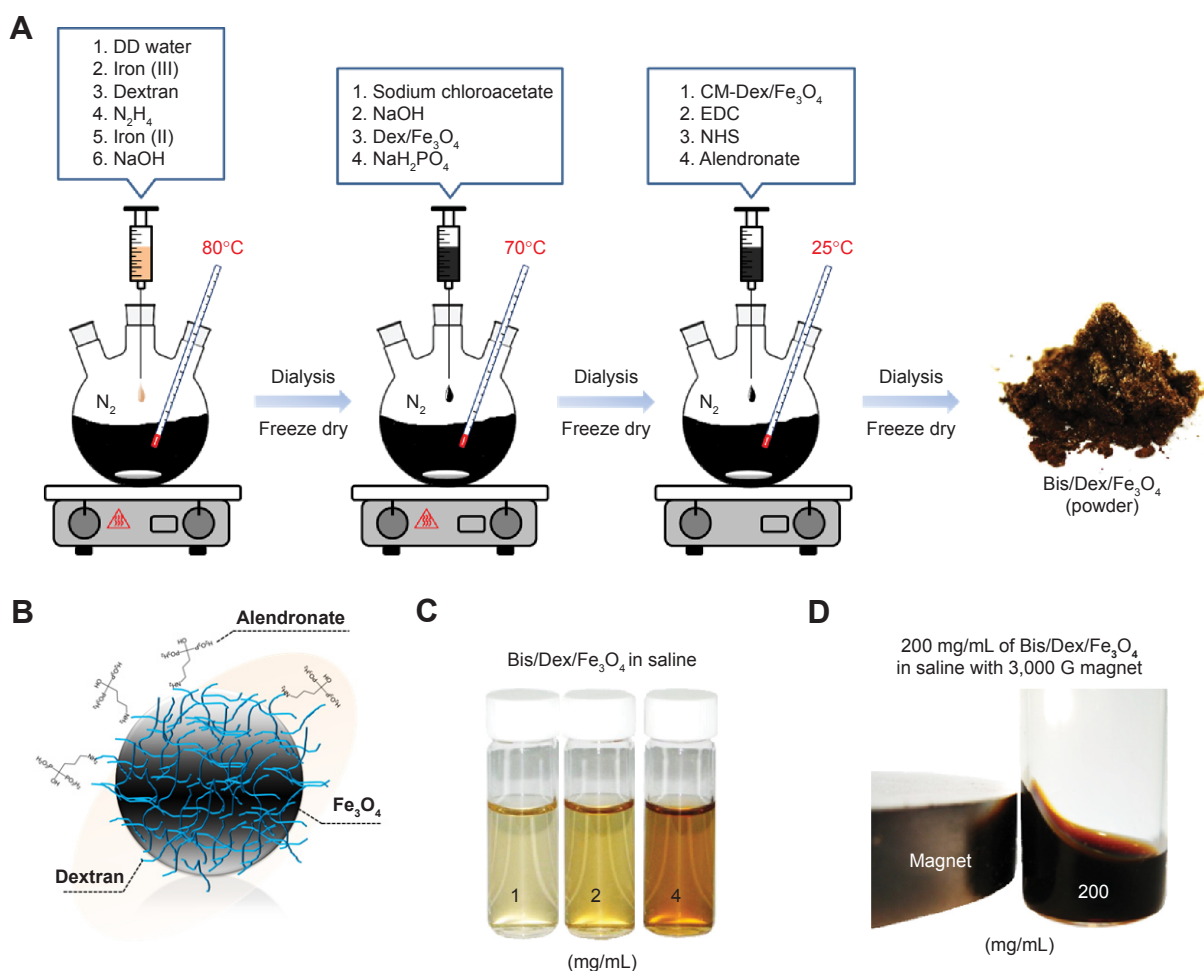
Figure 1 Synthesis scheme of magnetic nanoparticles and the final product.
Notes: (**A**) The procedure for synthesizing three different types of magnetic nanoparticles: Fe_3O_4, Dex/Fe_3O_4, and $Bis/Dex/Fe_3O_4$. (**B**) The scheme of the final product $Bis/Dex/Fe_3O_4$. (**C**) $Bis/Dex/Fe_3O_4$ fully dispersed in PBS at concentrations of 1, 2, and 4 mg/mL (from left to right). (**D**) High concentration (200 mg/mL) of $Bis/Dex/Fe_3O_4$ magnetic nanoparticles are well dispersed in the saline and attracted by a 3,000 G magnet.
Abbreviations: Fe_3O_4, iron (II, III) oxide; Dex, dextran; Bis, bisphosphonate; PBS, phosphate-buffered saline; DD, double-distilled; N_2H_4, hydrazine; NaOH, sodium hydroxide; NaH_2PO_4, sodium phosphate monobasic; EDC, 1-ethyl-3-(3-dimethylaminopropyl) carbodiimide; NHS, N-hydroxysuccinimide.

increase particle saturation magnetization. After 5 minutes, a mixture of ferrous chloride tetrahydrate and double-distilled water was injected into flask. After the solution was mixed completely, 8 mL of 1 N sodium hydroxide was slowly dropped at a speed of 0.3 mL/min into the mixture as a precipitant. The products were cooled to room temperature, and the mixture containing redundant iron cation, Dex, hydrazine, and sodium hydroxide that did not participate in the reaction was removed by a 50,000 Da cut-off dialysis membrane (Spectra/Por® 6 dialysis membrane; Spectrum Laboratories, Inc., Rancho Dominguez, CA, USA). The final black product, Dex/Fe_3O_4, was obtained by freeze-drying.

Preparation of CM-Dex/Fe₃O₄ magnetic nanoparticles

In the previous process, the Dex/Fe_3O_4 were prepared by a chemical co-precipitation method (Figure 1A, middle).

For carboxyl surface modification of Dex/Fe_3O_4, 10 mg of sodium chloroacetate and 10 mg of Dex/Fe_3O_4 were added to 10 mL of 3 M sodium hydroxide at 70°C with mechanical stirring for 1 hour. Then, 120 mg of sodium phosphate dibasic was added to the reaction mixture for 10 minutes, and the pH was adjusted to 7.2 by hydrochloric acid. After the products were cooled to room temperature, the redundant chemicals that did not participate in the reaction were removed by ~50,000 Da cut-off dialysis membrane. The final black product, $COOH-Dex/Fe_3O_4$ ($CM-Dex/Fe_3O_4$), was obtained by freeze-drying.

Preparation of Bis/Dex/Fe₃O₄ magnetic nanoparticles

Alendronate, a nitrogen-containing Bis, was covalently attached to $CM-Dex/Fe_3O_4$ using EDC and NHS (Figure 1A, right). One milligram of $CM-Dex/Fe_3O_4$, 60 mM EDC, and 15 mM NHS were mixed in double-distilled water at room temperature

for 1 hour. Next, 15 mM Bis was added into the solution and mixed for 24 hours. Redundant chemicals were removed using a 50,000 Da cut-off dialysis membrane to isolate the Bis/Dex/Fe_3O_4 magnetic nanoparticles (Figure 1B–D).

Characterization of magnetic nanoparticles

The functional groups on the particles were identified by Fourier transform infrared (FT-IR) spectroscopy using a JASCO IR-4200 (JASCO Inc, Easton, MD, USA). The percentage of Dex and alendronate that were coated onto the nanoparticles was identified by thermogravimetric analysis (TGA) using a Mettler TGA/SDTA 851 (Mettler Toledo, Columbus, OH, USA). The samples were prepared using potassium bromide powder. The Dex-coated magnetic nanoparticles were determined by field emission gun scanning electron microscopy (SEM) using a Quanta 400 FEG (FEI, Hillsboro, OR, USA). The particles' inner morphology and size distribution were analyzed by transmission electron microscopy (TEM) using a JEOL TEM-3010 (Nanolab Technologies, Milpitas, CA, USA). The nanoparticle samples were prepared via embedding in epoxy and slicing to 80 nm thickness on a carbon-coated copper coil. The crystal structure was identified by powder X-ray diffraction (XRD) using a Panalytical X'Pert Pro X PW3040/60 (PANalytical, Almelo, Netherlands). Superparamagnetism was observed by superconducting quantum interference device (SQUID) magnetometer using a Quantum Design MPMS5 (Quantum Design, Inc., San Diego, CA, USA) in a field ranging from 0 to 10 kOe at room temperature.

RF system

A high-frequency induction-heating machine (Kanwei machine & Tool agent CO., LTD) (happy GP-15A; New Taipei City, Taiwan) composed of a power supply (power source 15 kVA, output frequency 42 kHz, heating current 450 A), coil, and chiller was used. The temperature was measured by a FOT Lab Kit fiber optic thermometer (LumaSense Technologies, Inc. Santa Clara, CA, USA) every second at humidified atmosphere containing 5% CO_2 (Figure 2A). The temperature of the three types of nanoparticles (at high and low concentration) was recorded under RF exposure.

Cell culture and viability assay

All cells were purchased from American Type Culture Collection (ATCC) (Manassas, VA, USA) and grown on tissue culture polystyrene at 37°C under 5% CO_2.

MC3T3-E1 osteoblast (OB) cells were cultured in DMEM with 10% fetal bovine serum, 100 U/mL penicillin, and

100 U/mL streptomycin. Experiments began 24 hours after cell plate seeding. RAW264.7 mouse macrophages as OC precursors were cultured in DMEM with 10% fetal bovine serum, 100 U/mL penicillin, and 100 µg/mL streptomycin at a density of 10^4 cells/well in a 24-well culture plate. The cells were cultured with a fresh medium containing RANKL at 100 ng/mL and replaced every 2 days. Experiments began 6 days after cell seeding (Figure 2B). OB- and OC-like cells were cultured with different composite nanoparticles (Fe_3O_4, Dex/Fe_3O_4, and Bis/Dex/Fe_3O_4) at 1 mg/mL. After 24 hours, the magnetic nanoparticles were removed by replacing the medium and exposing the cells to RF for 20 minutes. Cells were returned to the incubator for 24 hours, and MTT viability assay was performed.

Cell viability was determined by MTT assay in which yellow tetrazole was reduced to purple crystals in living cells. The OB- and OC-like cells were exposed to 20 minutes of RF and then cultured for 24 hours. One hundred microliters of MTT solution was directly added into the culture medium. The plate was incubated for 4 hours in the dark at 5% CO_2, and 100 µL of dimethyl sulfoxide was substituted for the MTT solution to dissolve the formazan into purple solution. The optical density was measured at 570 nm with an enzyme-linked immunosorbent assay reader (1500-490; Thermo Fisher Scientific, Waltham, MA, USA).

In vivo animal experiments

All animals were obtained from BioLASCO Co. (Taipei, Taiwan). Fifteen male Wistar rats aged 7–8 weeks were used in the experiment. They were housed in 12-hour light/dark cycles at 25°C. Animals were separated into groups of three per cage with food and tap water ad libitum.

The superparamagnetism of iron oxide nanoparticles makes them an excellent image contrast tool for MRI. In order to verify the effects of composite nanoparticles Dex/Fe_3O_4 on the MRI, we proposed to test them as contrast agents in vitro and in vivo, respectively. For in vitro tests, the magnetic nanoparticles Dex/Fe_3O_4 were added to the culture plate at different concentrations such as 0, 12.5, 25, 50, 100, 150, and 200 µg/mL. The T2-MRI was performed using a clinical 7 T magnetic resonance scanner with a repetition time of 750 ms and an echo time of 14 ms. The in vivo tests were done using a clinical 1.5 T magnetic resonance scanner with a repetition time of 200 ms, an echo time of 95 ms, and a field of view of 12×12 cm. The Wistar rats were injected with the magnetic nanoparticles Bis/Dex/Fe_3O_4 at a concentration of 1 mg/mL. Furthermore, the T2-MRI was done at different periods: 0 (before injection), 15, and 30 minutes (Figure 3B).
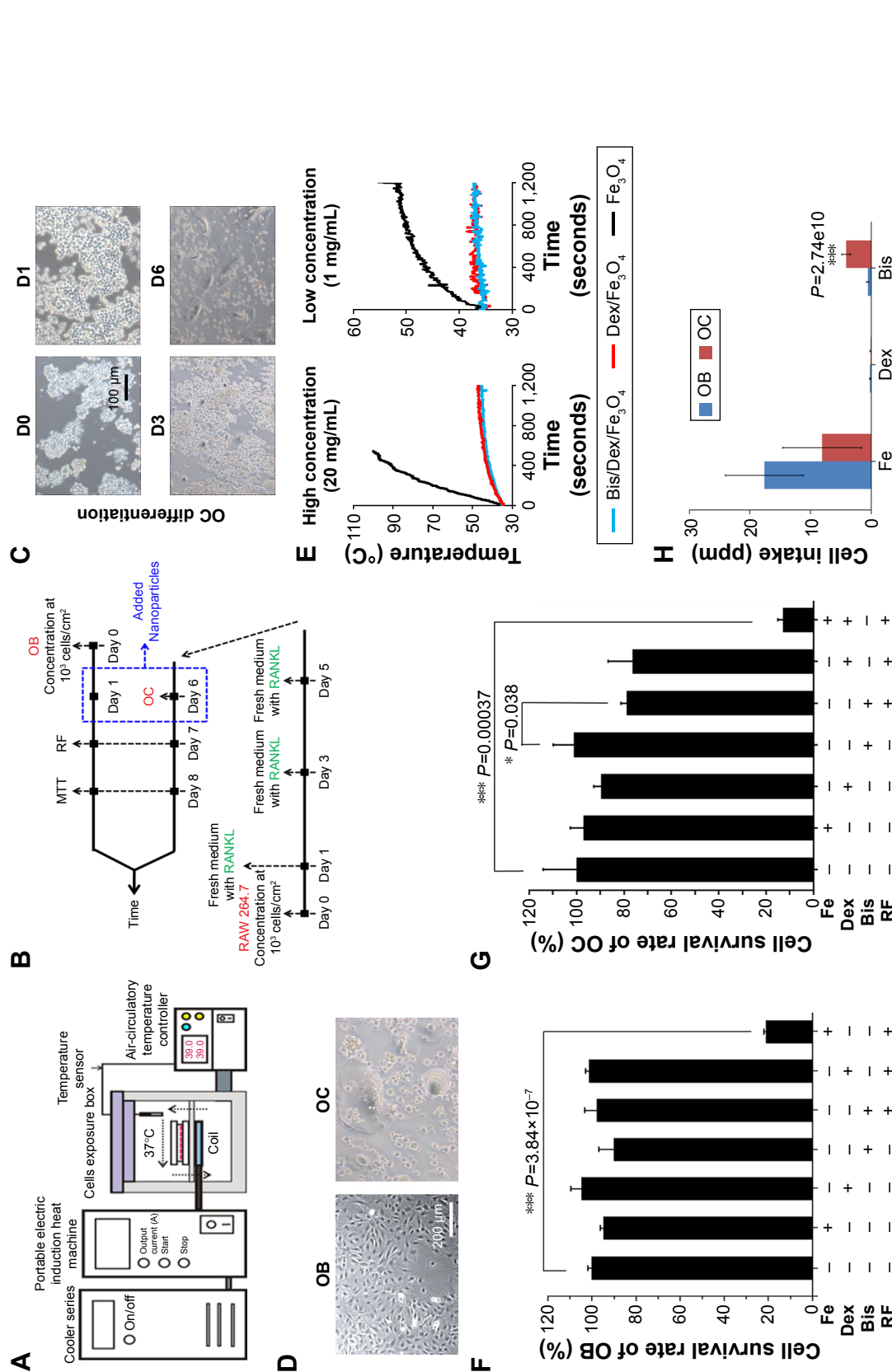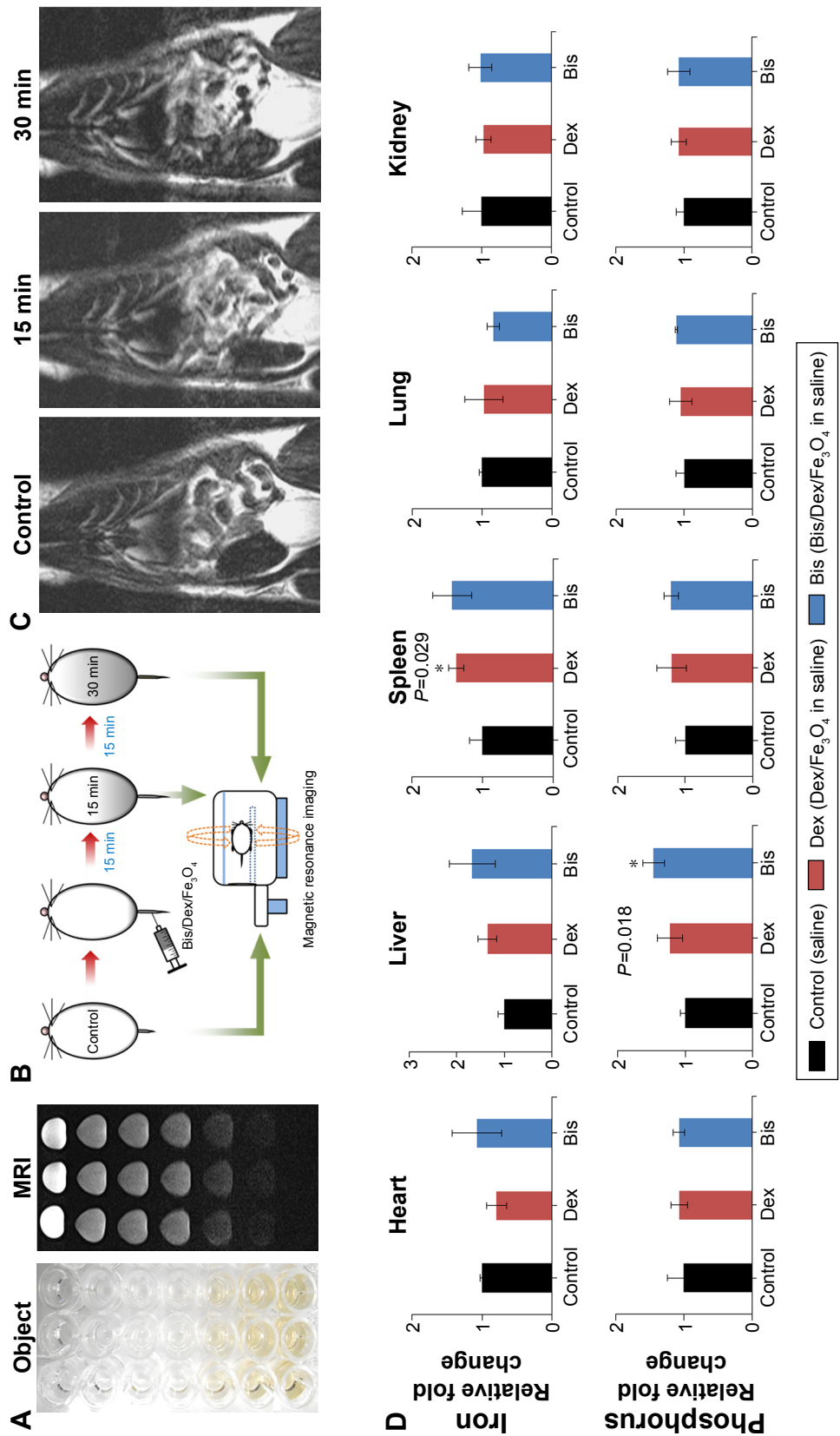
Figure 2 In vitro cell survival rate of OBs and OCs cultured with three different nanoparticles.

Notes: (**A**) A schematic diagram of RF system with an air circulation temperature controller. (**B**) Experimental procedure of OC differentiation, OB and OC exposure to RF, and cell survival rate examination. (**C**) Cell morphology of RAW 264.7 when differentiated into OCs from days 0 to 6. Scale bar: 200 μm. (**D**) Cell morphology of OBs and OCs at day 6. Scale bar: 100 μm. (**E**) The variation of temperature at low (1 mg/mL) and high (20 mg/mL) concentration of Fe$_3$O$_4$, Dex/Fe$_3$O$_4$, and Bis/Dex/Fe$_3$O$_4$ magnetic nanoparticles under RF exposure. (**F**) The cell survival rate of OBs cultured under seven different conditions – with no nanoparticles and RF, with Fe$_3$O$_4$, with Dex/Fe$_3$O$_4$, with Bis/Dex/Fe$_3$O$_4$, with Dex/Fe$_3$O$_4$ under RF, with Dex/Fe$_3$O$_4$ under RF, and with Fe$_3$O$_4$ under RF. Significant decrease in cell survival rate when OBs are cultured with Fe$_3$O$_4$ under RF exposure (P=3.84×10⁻⁷). (**G**) The cell survival rate of OCs cultured under seven different conditions – with no nanoparticles and RF, with Fe$_3$O$_4$, with Dex/Fe$_3$O$_4$, with Bis/Dex/Fe$_3$O$_4$, with Bis/Dex/Fe$_3$O$_4$ under RF, with Dex/Fe$_3$O$_4$ under RF, and with Fe$_3$O$_4$ under RF. Significant difference between Bis/Dex/Fe$_3$O$_4$ without and Bis/Dex/Fe$_3$O$_4$ with RF exposure (P=0.038), and Fe$_3$O$_4$ without and Fe$_3$O$_4$ with RF exposure (P=3.7×10⁻⁴). (**H**) Cell intake of OBs and OCs cultured with Fe$_3$O$_4$, Dex/Fe$_3$O$_4$, and Bis/Dex/Fe$_3$O$_4$. *P<0.05, ***P<0.001.

Abbreviations: OBs, osteoblasts; OCs, osteoclasts; RF, radiofrequency; Fe$_3$O$_4$, iron (II, III) oxide; Dex, dextran; Bis, bisphosphonate; MTT, 3-(4,5-dimethylthiazol-2-yl)-2,5-diphenyltetrazolium bromide; RANKL, receptor activator of nuclear factor kappa-B ligand; OC, osteoclast.

Figure 3 MRI scans and accumulation amount after injection of Bis/Dex/Fe$_3$O$_4$ magnetic nanoparticles.
Notes: (**A**) Bis/Dex/Fe$_3$O$_4$ magnetic nanoparticles under the MRI as contrast agents at different concentrations from top to bottom: 0, 12.5, 25, 50, 100, 150, and 200 µg/mL. (**B**) The experimental process of MRI in vivo test. Same rat was setting up to do the series exam from control to Bis/Dex/Fe$_3$O$_4$ injection 15, and 30 minutes. (**C**) MRI scans of the rat were taken after injections at 0, 15, and 30 minutes. (**D**) Magnetic nanoparticles accumulation in the animal heart, liver, spleen, lung, and kidney. These organs were harvested 24 hours after magnetic nanoparticles injection. *$P<0.05$.
Abbreviations: MRI, magnetic resonance imaging; Bis, bisphosphonate; Dex, dextran; Fe$_3$O$_4$, iron (II, III) oxide; min, minutes.

Kinetics of magnetic nanoparticles accumulation

In the in vitro accumulation study, Fe_3O_4, Dex/Fe_3O_4, and $Bis/Dex/Fe_3O_4$ were cultured with OBs and OCs for 24 hours. After 24 hours, the culture medium was washed twice by PBS. After that, the cells were lysed by 100% nitrate solution. The iron quantity was detected by the inductively coupled plasma-mass spectrometry (ICP-MS).

To investigate the localization of nanoparticles in the body, animal models were used to verify the concentration in different organs. Animals were divided into two groups: control and 24 hours after injection (n=4). After the animals were sacrificed, the heart, liver, spleen, lung, kidney, and bone were taken out and directly dissolved in 100% nitrate solution. The organs were tested for iron and phosphorus concentrations by ICP-MS.

Statistical analysis

All in vitro tests were performed in triplicates (n=3), and in vivo tests in quadruplicates (n=4). Data are presented as the mean ± standard deviation. Differences between groups were analyzed using paired t-tests, and a one-way analysis of variance was used to compare different groups. A P-value of <0.05 was considered statistically significant.

Results
Characterization of Fe_3O_4, Dex/Fe_3O_4, and $Bis/Dex/Fe_3O_4$

The $Bis/Dex/Fe_3O_4$ nanoparticles looked like cotton after being freeze-dried (Figure 1A). According to the proposed model, both Dex and Bis were coated or twined and grafted onto Fe_3O_4 (Figure 1B). The $Bis/Dex/Fe_3O_4$ nanoparticles in resuspension were dispersed in the double-distilled water (Figure 1C). Furthermore, after the magnetic nanoparticles at high concentrations were dissolved in water, the solution became magnetized (Figure 1D).

The functional groups on the material surface were analyzed using FT-IR spectroscopy (Figure 4A). Since Dex is a glucose polymer, it contains carbon, hydrogen, and oxygen atoms. Dex coating onto Fe_3O_4 was shown by the presence of 1,010 (carbon–hydrogen bond) and 2,918 cm^{-1} (carbon–oxygen bond) signals, which were absent in the spectrum of Fe_3O_4. The formula of Bis is $C_4H_{12}NNaO_7P_2\cdot3H_2O$. Grafting of Bis onto Dex/Fe_3O_4 was shown by the absorption wavelengths at 1,114 (amino bond) and 2,356 cm^{-1} (carbon–nitrogen bond), which were absent in the spectrum of Dex/Fe_3O_4. These data suggest that Bis and Dex were successfully incorporated onto Fe_3O_4

molecules. The lattice structure of Fe_3O_4, Dex/Fe_3O_4, and $Bis/Dex/Fe_3O_4$ was verified by XRD (Figure 4B). Lattice planes represented by the diffraction peak at angles of 30.18°, 35.56°, 43.22°, 53.62°, 57.14°, and 67.20° were, respectively, (220), (311), (400), (422), (511), and (440); the results are in complete agreement with the standard Fe_3O_4 pattern published by JCPDS. The peak patterns represented the diffracted light intensities of the lattice planes. It was inferred that the relative peak of Dex/Fe_3O_4 and $Bis/Dex/Fe_3O_4$ was smaller than that of Fe_3O_4 because Dex and Bis have noncrystalline structure; thus, the diffraction peaks were disturbed and weakened. Even though the peaks were weakened because of the coating, their corresponding lattice planes still represented Fe_3O_4. This suggests that the chemical modification did not affect the lattice structure of the material. In addition to lattice structure, XRD also provided an estimate of the size of the $Bis/Dex/Fe_3O_4$ nanoparticles using Scherrer's equation. SQUID magnetometer was used to detect the saturation magnetization of the nanoparticles (Figure 4C). The saturation magnetizations of Fe_3O_4, Dex/Fe_3O_4, and $Bis/Dex/Fe_3O_4$ were, respectively, 81.7, 22.7, and 18.2 emu/g, which exceeds the data found in previous literature and thus increases the feasibility for biomedical and clinical application. Coating Bis and Dex onto Fe_3O_4 dropped the saturation magnetization significantly. Previous XRD results had excluded the possibility of changes in lattice structure; thus, a possible reason could be that the distance between particles caused by the Dex coating enhances dispersion and reduces coagulation; this leads to the formation of a core–shell structure, which causes significant magnetization drop. In addition, the results showed that all composite nanoparticles were superparamagnetic, which could be used for MRI. The content of Dex and Bis on the Fe_3O_4 was confirmed by TGA. Five samples remained separately even after the temperature reached 600°C: 95% of Fe_3O_4, 10.8% of Dex, 29.3% of Dex/Fe_3O_4, 54.4% of Bis, and 43.45% of $Bis/Dex/Fe_3O_4$ (Figure 4D). There are two points worth mentioning: one is the percentage of Dex coated on the Fe_3O_4, and the other is the percentage of Bis grafted on the Dex/Fe_3O_4. The Dex/Fe_3O_4 contained 78.9% Dex and 21.1% Fe_3O_4. In other words, the ratio of Dex to Fe_3O_4 was 3.74 to 1. $Bis/Dex/Fe_3O_4$ contained 56.4% Bis, 34.4% Dex, and 9.2% Fe_3O_4, which means the ratio of Bis to Dex to Fe_3O_4 was 6.13 to 3.74 to 1.

Surface structure of Dex/Fe_3O_4 and $Bis/Dex/Fe_3O_4$ was analyzed by SEM (Figure 5A and B) and TEM (Figure 5C and D). Both nanoparticles had a relatively rough surface but still had a similar shape as commercial Dex (data not shown).
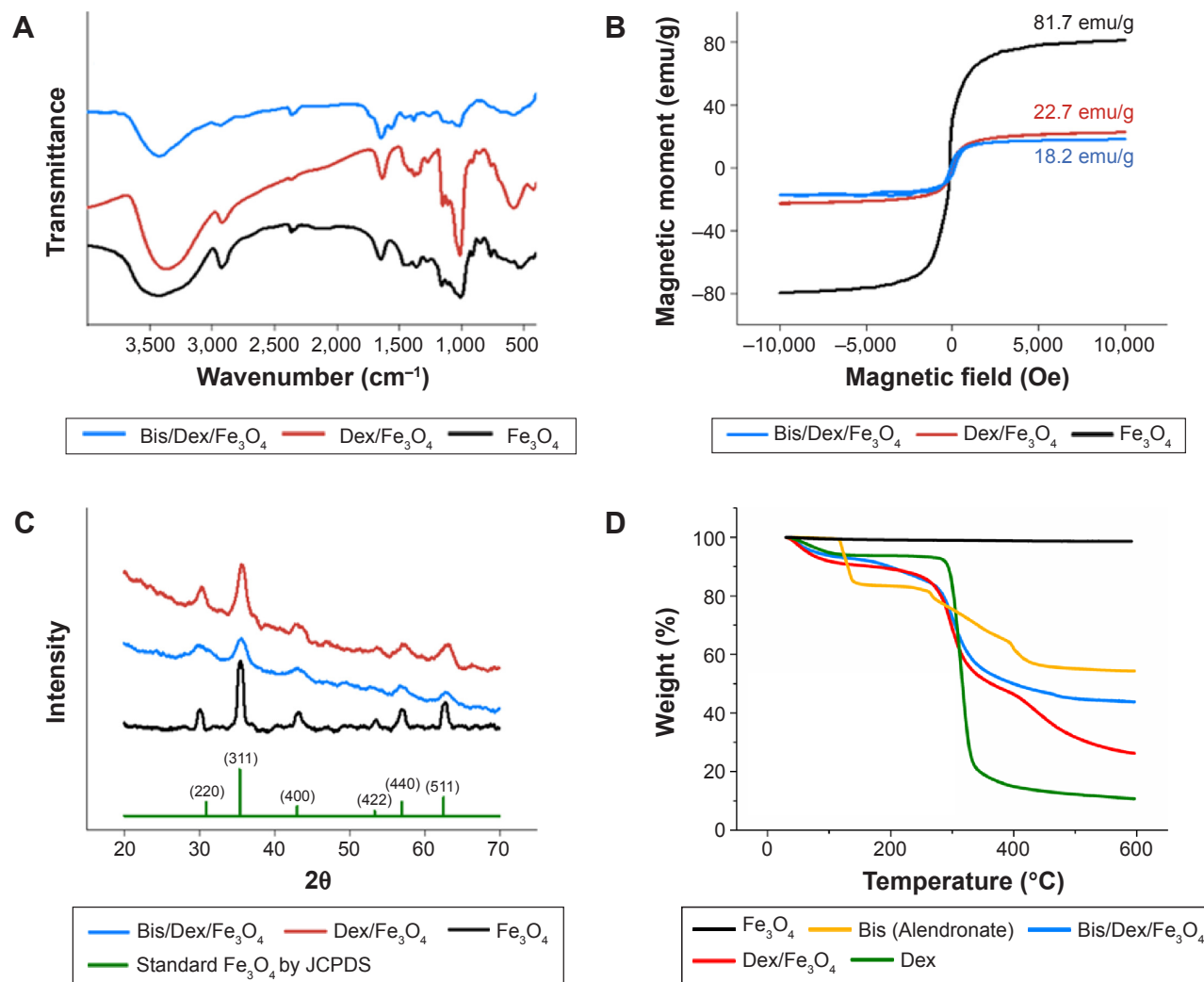
Figure 4 Physical and chemical characterization of Fe_3O_4, Dex/Fe_3O_4, and $Bis/Dex/Fe_3O_4$.
Notes: (**A**) FT-IR spectroscopy transmittance peak values show the components of the magnetic nanoparticles. Dex coating onto Fe_3O_4 is shown by the presence of carbon–hydrogen bond (1,010 cm^{-1}). Grafting of Bis onto Dex/Fe_3O_4 is shown by the presence of amino bond (1,114 cm^{-1}) and carbon–nitrogen bond (2,356 cm^{-1}). (**B**) Magnetic strength of nanoparticles as measured by SQUID magnetometer. 81.7, 22.7, and 18.2 emu/g are the saturation magnetization of Fe_3O_4, Dex/Fe_3O_4, and $Bis/Dex/Fe_3O_4$, respectively. (**C**) Lattice structure of all three types of the magnetic nanoparticles as shown by XRD. The diffraction peaks at 30.18°, 35.56°, 43.22°, 53.62°, 57.14°, and 67.20° are, respectively, (220), (311), (400), (422), (511), and (440). (**D**) The relative drug content on the nanoparticle is shown by TGA. The Dex/Fe_3O_4 contains 78.9% of Dex and 21.1% of Fe_3O_4. The $Bis/Dex/Fe_3O_4$ contains 56.4% of Bis, 34.4% of Dex, and 9.2% of Fe_3O_4.
Abbreviations: Fe_3O_4, iron (II, III) oxide; Dex, dextran; Bis, bisphosphonate; FT-IR, Fourier transform infrared; SQUID, superconducting quantum interference device; XRD, X-ray diffraction; TGA, thermogravimetric analysis.

A close observation (Figure 5A-1 and B-1) revealed that the rough surface comprised granular bulges. The particles' size measured by TEM was ~20 nm, which is in agreement with previous results.

When the magnetic nanoparticles were exposed to RF, the temperature change was recorded by a fiber thermometer (Figure 2E). At low concentrations (1 mg/mL), both Dex/Fe_3O_4 and $Bis/Dex/Fe_3O_4$ showed little response after 20 minutes of RF exposure. On the other hand, the temperature increased to ~50°C for Fe_3O_4. At high concentrations (20 mg/mL), Dex/Fe_3O_4 and $Bis/Dex/Fe_3O_4$ increased temperature by 7°C, and Fe_3O_4 by >100°C, after 20 minutes of RF exposure.

Cell survival rate
Photos of OCs and OBs were taken on days 0, 1, 3, and 6 (Figure 2C and D).

Three different magnetic nanoparticles were cultured with OBs. After 24 hours of culture, the magnetic nanoparticles were removed by replacing the medium and exposing the cells to RF for 20 minutes. The cells were continuously cultured for another 24 hours, and then tested for cell viability using MTT assay (Figure 2F). The results showed that Dex coating effectively enhanced the biocompatibility of magnetic nanoparticles and the grafted Bis had no cytotoxicity. There was no difference in viability between the RF- and non-RF-treated OBs (data not shown),
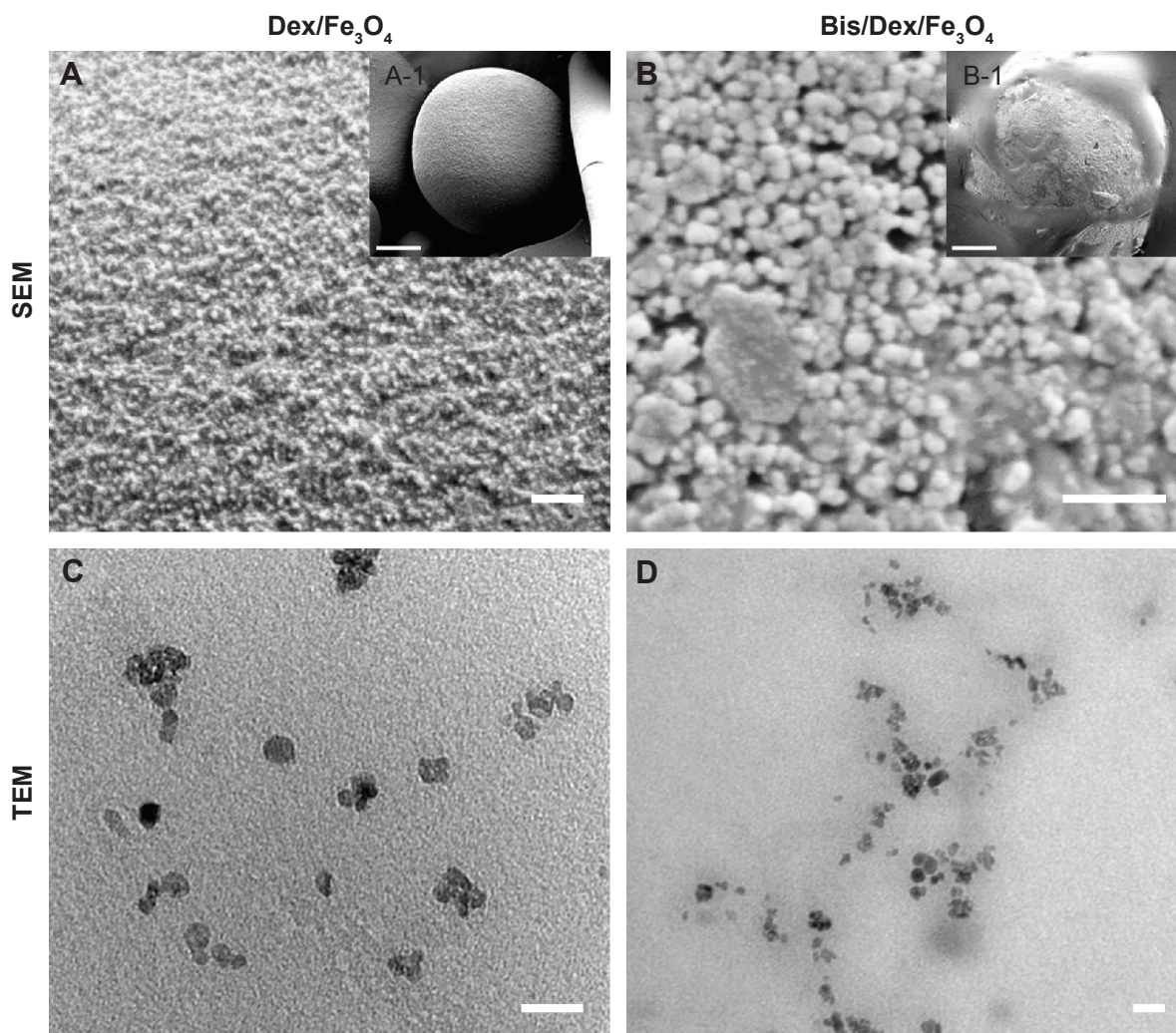
Figure 5 The SEM and TEM images of Dex/Fe$_3$O$_4$ and Bis/Dex/Fe$_3$O$_4$.
Notes: (**A** and **A-1**) SEM image of the Dex/Fe$_3$O$_4$ indicates the magnetic nanoparticles on the Dex surface. (**B** and **B-1**) The morphology of Bis/Dex/Fe$_3$O$_4$ under SEM. (**C** and **D**) Dex/Fe$_3$O$_4$ and Bis/Dex/Fe$_3$O$_4$ nanoparticles photographed by TEM show an approximate size of 20 nm. Scale bar: (**A**) 500 nm, (**A-1**) 5 µm, (**B**) 500 nm, (**B-1**) 5 µm, (**C**) 20 nm, and (**D**) 20 nm.
Abbreviations: SEM, scanning electron microscopy; TEM, transmission electron microscopy; Dex, dextran; Fe$_3$O$_4$, iron (II, III) oxide; Bis, bisphosphonate.

indicating that the radiation produced no direct harm to OBs. The cell survival rate of the Fe$_3$O$_4$ cultured with OBs was reduced to approximately 15% ($P<0.001$, designated with ***) when compared with the control group. On the other hand, OBs cultured with Dex/Fe$_3$O$_4$ or Bis/Dex/Fe$_3$O$_4$ and exposed to RF showed no significant difference from the control group.

OCs were also cultured with the three types of nanoparticles for 24 hours in fresh medium, and exposed to RF for 20 minutes. After that, they were cultured for another 24 hours, and tested for cell viability using the MTT assay (Figure 2G). The cell survival rate of OCs cultured with the three nanoparticles was ~90%–100% with no significant difference compared to the control group. OCs cultured with Fe$_3$O$_4$ and exposed to RF showed a decrease in viability to 10% ($P=0.00037$, designated with ***), but with

Bis/Dex/Fe$_3$O$_4$, the viability only reduced to ~80% ($P=0.038$, designated with *). Although there was a slight decrease in the OCs cultured with Dex/Fe$_3$O$_4$ under RF exposure, there was no significant difference between the Dex/Fe$_3$O$_4$ group (no RF) and the control group.

Bis/Dex/Fe$_3$O$_4$ nanoparticles under MRI
In vitro test
Different concentrations of Bis/Dex/Fe$_3$O$_4$ – 0, 12.5, 25, 50, 100, 150, and 200 µg/mL from top to bottom – were placed in the cell culture dish (Figure 3A, left) and subjected to MRI (Figure 3A, right). The results showed that with increasing particle concentration, the negative contrast signal increased (turned black). This suggests that Bis/Dex/Fe$_3$O$_4$ could be a good contrast agent for imaging during therapy.

In vivo test

To test the application of Bis/Dex/Fe_3O_4 magnetic nanoparticles in clinical medicine as a contrast agent, 1 mg/mL of the nanoparticles was injected into 8-week-old Wistar rats and imaged at 15 and 30 minutes (Figure 3C). The results showed that injection of the nanoparticle created higher imaging contrast and sharpness, particularly for the rat liver. Previous studies have shown that magnetic nanocomposite particles tend to accumulate in the liver, which is consistent with the results of this study.

Accumulation of Dex/Fe_3O_4 and Bis/Dex/Fe_3O_4 nanoparticles

The levels of iron were detected in OBs and OCs after 24 hours of culturing with the three nanoparticles. Comparable results were obtained for the Fe_3O_4 and Dex/Fe_3O_4 group. Surprisingly, a higher quantity of Bis/Dex/Fe_3O_4 was engulfed by OCs (P=2.74e10) (Figure 2H).

The amount of nanoparticles accumulated in the rats' organ was measured after injection of control (saline), Dex (Dex/Fe_3O_4), and Bis (Bis/Dex/Fe_3O_4) (Figure 3D). Twenty-four hours after the intravenous injection into the rat tail, Dex/Fe_3O_4 nanoparticles accumulated in large quantities in the spleen. There was no significant difference in the liver when compared to the control group. On the other hand, Bis/Dex/Fe_3O_4 nanoparticles accumulated in the liver after 24 hours of injection.

Discussion

Human skeleton relies on bone remodeling to maintain its strength.[32] This metabolic process occurs when aged bone tissues are resorbed by OCs and replaced by OBs.[33] However, in cases of significant bone loss such as osteoporosis, the resorption of aged bones exceeds the formation of new bones.[34] This study aimed to reduce OC activity by heating magnetic nanoparticles within the cells after OCs swallow them.

In this study, we synthesized Fe_3O_4, Dex/Fe_3O_4, and Bis/Dex/Fe_3O_4 that were able to increase local temperature for OC regulation. Grafting Dex to Fe_3O_4 increased Fe_3O_4 dispersion in aqueous environments. Alendronate is one of many Bis which are used to treat osteoporosis.[35–37] Grafting Bis onto magnetic nanoparticles increases the particle affinity to bone surfaces. Alendronate, also called (4-amino-1-hydroxy-1-phosphonobutyl) phosphonic acid, contains two major functional parts: an amino group and a Bis group. The amino group is able to inhibit OC activity, but it may introduce side effects like nausea, vomiting, and abdominal discomfort. As a result, we inactivated the amino group by grafting it with

Dex/Fe_3O_4 using the EDC–NHS crosslinking reaction. The Bis group, on the other hand, has high affinity to the calcium on skeletal surfaces. Consequently, the grafted nanoparticles were also able to adhere to bone. Our hypothesis is that the OCs will phagocytose Bis/Dex/Fe_3O_4 on the bone surface and thermalize by the RF induction. FT-IR spectroscopy showed that both Dex and Bis were successfully incorporated onto Fe_3O_4 particles. XRD revealed Fe_3O_4's cubic inverse spinel structure and that incorporation of the drugs did not alter its physical properties. SQUID magnetometer measurement also confirmed that the magnetic strength did not diminish after grafting Dex and Bis. Furthermore, the results indicated that all the three composite nanoparticles had no magnetic hysteresis. Consequently, these superparamagnetic nanoparticles could be used as MRI contrast agents, or single-cell trackers. We established that the size of the nanoparticle was ~23 nm with beaded surface. Due to the particle similarity, we were not able to differentiate between Dex/Fe_3O_4 and Bis/Dex/Fe_3O_4 under SEM. The capability of nanoparticles to rise their temperature under the RF exposure was measured by a fiber optic thermometer. One possible reason for the small temperature increase by Dex/Fe_3O_4 and Bis/Dex/Fe_3O_4 is the low levels of iron. This result is also consistent with TGA measurements, which also indicated that the Dex/Fe_3O_4 and Bis/Dex/Fe_3O_4 only contained 21.1% and 9.2% of iron, respectively. However, once we increased the concentration to 20 mg/mL, the rate of temperature change exceeded 7°C in 20 minutes. We conclude that the change in temperature is directly correlated with the levels of Fe_3O_4 in the medium.

Since OB and OC cells both reside on bone surface, there is a concern that OBs will also engulf the nanoparticles and thermalize from the RF. Thus, the survival rates of both cell types were investigated. The cell viability assays pointed out significantly lower cell survival rates of OCs when cultured with Bis/Dex/Fe_3O_4 and subjected to RF exposure. When Fe_3O_4 was cultured with OBs and OCs under RF exposure, the cell survival rate declined to ~20%. The reason for this is that aggregation of Fe_3O_4 will overheat the cells when exposed to RF. However, coating the material greatly attenuates the increase in temperature. For example, exposure of Bis/Dex/Fe_3O_4 to RF did not decrease the survival rate of OB but decreased that of OC to 80% (P=0.038, designated with *). Notwithstanding is the fact that the effect of RF on temperature rise of Bis/Dex/Fe_3O_4 could not be measured with a fiber optic thermometer mainly because prior to cell RF radiation, excess materials (not taken in by the cells) had been rinsed and removed with PBS, causing very little change

in water temperature measurements. This suggests a difference in heat tolerance between OBs and OCs. We further intended to investigate the cell intake in both OBs and OCs. The cell intake and nanoparticles accumulated in rat quantity were verified by ICP-MS. According to the elemental composition of nanoparticles, iron and phosphorus were selected to measure the accumulation quantity. As a result, Bis facilitated endocytosis by OCs to engulf the nanoparticles of Bis/Dex/Fe$_3$O$_4$. Based on this result, OCs engulfed more Bis/Dex/Fe$_3$O$_4$ than OBs, which suggests that OCs had more nanoparticles exposed to RF. This is the reason that the cell survival rate of OBs is higher than that of OCs. Cell-specific thermolysis could be advantageous for rebalancing bone homeostasis because it can reduce the growth of OCs without damaging the microenvironment. Long-term treatments with the nanoparticle could potentially limit and reverse the osteoporotic phenotype.

We were concerned that the structure of the final product Bis/Dex/Fe$_3$O$_4$ will be changed during the synthesis process, so its function as an MRI contrast agent was tested. The superparamagnetism of the particles can enhance the r_2 relativity to decrease the targeted signal.[38] SQUID magnetometer and MRI measurements showed that the final product still maintained its material behavior and capacity to be a contrast agent in MRI. The accumulation data from previous literature are consistent with our results, as they have demonstrated that large quantities of magnetic nanoparticles still remained in the liver and spleen 24 hours after injection.

Finally, all experimental rats lived after treatment with the nanoparticle, illustrating biocompatibility. This study successfully developed magnetic nanoparticles that are effective in controlling osteoporosis by thermolysis of OC. The difference in thermal resistance between OBs and OCs was also verified individually. In the future, we will apply Bis/Dex/Fe$_3$O$_4$ to osteoporotic animals and further investigate the seletivity of nanoparticle-induced thermolysis when introduced to OB and OC transwell cultures.

Conclusion

We successfully synthesized Dex/Fe$_3$O$_4$ and Bis/Dex/Fe$_3$O$_4$ nanoparticles by the chemical co-precipitation method. In our in vitro study, OBs and OCs were both cultured with Bis/Dex/Fe$_3$O$_4$ nanoparticles under RF exposure. The results showed a significant decrease of cell survival rate in the OC group compared with that of the control and OB group. Furthermore, the in vivo study indicated that the nanoparticles of Bis group not only could be used as a nanomedicine but

also could be applied as a stable MRI contrast agent. For the purpose of controlling osteoporosis, this study developed a magnetic nanoparticle with water-dispersible, biocompatible, and RF-induced thermogenic properties. The results indicated that the Bis/Dex/Fe$_3$O$_4$ nanoparticle has the potential to contribute to osteoporosis treatment.

Disclosure

The authors report no conflicts of interest in this work.

References

1. National Osteoporosis Foundation. Available from: https://www.nof.org/patients/what-is-osteoporosis/. Accessed August 9, 2016.
2. Drake MT, Clarke BL, Kholsa S. Bisphosphonates: mechanism of action and role in clinical practice. *Mayo Clinic Proc*. 2008;83(9):1032–1045.
3. Boivin G, Doublier A, Farlay D. Strontium ranelate – a promising therapeutic principle in osteoporosis. *J Trace Elem Med Biol*. 2012;26(2–3):153–156.
4. Sambrook P, Birmingham J, Kelly P, et al. Prevention of corticosteroid osteoporosis: a comparison of calcium, calcitriol, and calcitonin. *N Engl J Med*. 1993;328(24):1747–1752.
5. Dempster DW, Lambing CL, Kostenuik PJ, Grauer A. Role of RANK ligand and denosumab, a targeted RANK ligand inhibitor, in bone health and osteoporosis: a review of preclinical and clinical data. *Clin Ther*. 2012;34(3):521–536.
6. Weinstein RS, Roberson PK, Manolagas SC. Giant osteoclast formation and long-term oral bisphosphonate therapy. *N Engl J Med*. 2009;360(16):53–62.
7. Burshell AL, Möricke R, Correa-Rotter R, et al. Correlations between biochemical markers of bone turnover and bone density responses in patients with glucocorticoid-induced osteoporosis treated with teriparatide or alendronate. *Bone*. 2010;46(4):935–939.
8. Sato H, Tanno K, Muro-oka G, Itai K. Serum ionic fluoride concentrations are significantly decreased after treatment with alendronate in patients with osteoporosis. *Clin Chim Acta*. 2011;412(23–24):2146–2149.
9. Rossini M, Gatti D, Girardello S, Braga V, James G, Adami S. Effects of two intermittent alendronate regimens in the prevention or treatment of postmenopausal osteoporosis. *Bone*. 2000;27(1):119–122.
10. Kendler D, Kung AWC, Fuleihan GEH, et al. Patients with osteoporosis prefer once weekly to once daily dosing with alendronate. *Maturitas*. 2004;48(3):243–251.
11. Lowe CE, Depew WT, Vanner SJ, Paterson WG, Meddings JB. Upper gastrointestinal toxicity of alendronate. *Am J Gastroenterol*. 2000;95(3):634–640.
12. Abdelmalek MF, Douglas DD. Alendronate-induced ulcerative esophagitis. *Am J Gastroenterol*. 1996;91(6):1282–1283.
13. Jiang W, Kim BY, Rutka JT, Chan WC. Advances and challenges of nanotechnology-based drug delivery systems. *Expert Opin Drug Deliv*. 2007;4(6):621–633.
14. Wang Y, Zhao Q, Han N, et al. Mesoporous silica nanoparticles in drug delivery and biomedical applications. *Nanomedicine*. 2015;11(2):313–327.

15. Oka C, Ushimaru K, Horiishi N, et al. Core–shell composite particles composed of biodegradable polymer particles and magnetic iron oxide nanoparticles for targeted drug delivery. *J Magn Magn Mater*. 2015;381:278–284.

16. Massart R. Preparation of aqueous magnetic liquids in alkaline and acidic media. *IEEE Trans Magn*. 1981;17(2):1247–1248.

17. Xie J, Lee S, Chen X. Nanoparticle-based theranostic agents. *Adv Drug Deliv Rev*. 2010;62(11):1064–1079.

18. Figuerola A, Corato RD, Manna L, Pellegrino T. From iron oxide nanoparticles towards advanced iron-based inorganic materials designed for biomedical applications. *Pharm Res*. 2010;62(2):126–143.

19. Daishun L, Michael JH, Taeghwan H. Surface ligands in synthesis, modification, assembly and biomedical applications of nanoparticles. *Nano Today*. 2014;9(4):457–477.

20. Lewis SL, Dirksen SR, Heitkemper MM, Bucher L. *Medical-Surgical Nursing: Assessment and Management of Clinical Problems*. 8th ed. Elsevier Health Sciences; Amsterdam, Netherlands; 2014.

21. Jordan A, Scholz R, Wust P, et al. Effects of magnetic fluid hyperthermia (MFH) on C3H mammary carcinoma in vivo. *Int J Hyperthermia*. 1997; 13(6):587–605.

22. Minamimura T, Sato H, Kasaoka S, et al. Tumor regression by inductive hyperthermia combined with hepatic embolization using dextran magnetite-incorporated microspheres in rats. *Int J Oncol*. 2000;16(6):1153–1158.

23. Lu AH, Salabas EL, Schüth F. Magnetic nanoparticles: synthesis, protection, functionalization, and application. *Angew Chem Int Ed*. 2007; 46(8):1222–1244.

24. Barry MA, Behnke CA, Eastman A. Activation of programmed cell death (apoptosis) by cisplatin, other anticancer drugs, toxins and hyperthermia. *Biochem Pharmacol*. 1990;40(10):2353–2362.

25. Vernon CC, Hand JW, Field SB, et al. Radiotherapy with or without hyperthermia in the treatment of superficial localized breast cancer: results from five randomized controlled trials. *Int J Radiat Oncol Biol Phys*. 1996;35(4):731–744.

26. Reichel E, Berrocal AM, Ip M, et al. Transpupillary thermotherapy of occult subfoveal choroidal neovascularization in patients with age-related macular degeneration. *Ophthalmology*. 1999;106(10):1908–1914.

27. Jordan A, Scholz R, Maier-Hauff K, et al. The effect of thermotherapy using magnetic nanoparticles on rat malignant glioma. *J Neurooncol*. 2006;78(1):7–14.

28. Maier-Hauff K, Rothe R, Scholz R, et al. Intracranial thermotherapy using magnetic nanoparticles combined with external beam radiotherapy: results of a feasibility study on patients with glioblastoma multiforme. *J Neurooncol*. 2007;81(1):53–60.

29. Blute ML, Tomera KM, Hellerstein DK, et al. Transurethral microwave thermotherapy for management of benign prostatic hyperplasia: results of the United States Prostatron Cooperative Study. *J Urol*. 1993;150 (5 Pt 2):1591–1596.

30. Jordan A, Maier-Hauff K. Magnetic nanoparticles for intracranial thermotherapy. *J Nanosci Nanotechnol*. 2007;7(12):4604–4606.

31. Gupta AK, Gupta M. Synthesis and surface engineering of iron oxide nanoparticles for biomedical engineering. *Biomaterials*. 2005;26(18):3995–4021.

32. Manolagas SC, Jilka RL. Bone marrow, cytokines, and bone remodeling – emerging insights into the pathophysiology of osteoporosis. *N Engl J Med*. 1995;332(5):305–311.

33. Katagiri T, Takahashi N. Regulatory mechanisms of osteoblast and osteoclast differentiation. *Oral Dis*. 2002;8(3):147–159.

34. Kanis JA, Melton LJ 3rd, Christiansen C, Johnston CC, Khaltaev N. The diagnosis of osteoporosis. *J Bone Miner Res*. 1994;9(8):1137–1141.

35. Liberman UA, Weiss SR, Bröll J, et al. Effect of oral alendronate on bone mineral density and the incidence of fractures in postmenopausal osteoporosis. *N Engl J Med*. 1995;333(22):1437–1444.

36. Bone HG, Hosking D, Devogelaer JP, et al. Ten years' experience with alendronate for osteoporosis in postmenopausal women. *N Engl J Med*. 2004;350(12):1189–1199.

37. Orwoll E, Ettinger M, Weiss S, et al. Alendronate for the treatment of osteoporosis in men. *N Engl J Med*. 2000;343(9):604–610.

38. Lee H, Lee E, Kim DK, Jang NK, Jeong YY, Jon S. Antibiofouling polymer-coated superparamagnetic iron oxide nanoparticles as potential magnetic resonance contrast agents for in vivo cancer imaging. *J Am Chem Soc*. 2006;128(22):7383–7389.